JOURNAL OF BACTERIOLOGY, Aug. 2008, p. 5663–5671 Vol. 190, No. 16
0021-9193/08/$08.00+0 doi:10.1128/JB.00346-08

The Compatible-Solute-Binding Protein OpuAC from *Bacillus subtilis*: Ligand Binding, Site-Directed Mutagenesis, and Crystallographic Studies▽

Sander H. J. Smits,[1]‡ Marina Höing,[2]‡ Justin Lecher,[1] Mohamed Jebbar,[3]†
Lutz Schmitt,[1]* and Erhard Bremer[2]

Institute of Biochemistry, Heinrich Heine University Düsseldorf, Universitätsstr. 1, 40225 Düsseldorf, Germany[1]; Laboratory for Microbiology, Department of Biology, Philipps University Marburg, Karl-von-Frisch Str., 35032 Marburg, Germany[2]; and Departement Osmoregulation chez les Bacteries, Universite de Rennes 1, UMR-CNRS 6026, Rennes, France[3]

Received 10 March 2008/Accepted 9 June 2008

In the soil bacterium *Bacillus subtilis*, five transport systems work in concert to mediate the import of various compatible solutes that counteract the deleterious effects of increases in the osmolarity of the environment. Among these five systems, the ABC transporter OpuA, which catalyzes the import of glycine betaine and proline betaine, has been studied in detail in the past. Here, we demonstrate that OpuA is capable of importing the sulfobetaine dimethylsulfonioacetate (DMSA). Since OpuA is a classic ABC importer that relies on a substrate-binding protein priming the transporter with specificity and selectivity, we analyzed the OpuA-binding protein OpuAC by structural and mutational means with respect to DMSA binding. The determined crystal structure of OpuAC in complex with DMSA at a 2.8-Å resolution and a detailed mutational analysis of these residues revealed a hierarchy within the amino acids participating in substrate binding. This finding is different from those for other binding proteins that recognize compatible solutes. Furthermore, important principles that enable OpuAC to specifically bind various compatible solutes were uncovered.

The soil bacterium *Bacillus subtilis* is equipped with five transport systems (Opu [*o*smo*p*rotectant *u*ptake]) that allow the import of a large number of compatible solutes (4, 5, 25). Compatible solutes are low-molecular-weight organic osmolytes that balance the osmotic potential of the cytoplasm with that of the environment. Three of the five compatible solute transport systems (OpuA, OpuC, and OpuD) mediate the uptake of the widespread-found osmoprotectant glycine betaine (22, 24). Glycine betaine can also be synthesized by *B. subtilis* from the precursor choline (3), which is acquired from the environment via the osmoregulated OpuB and OpuC transporters (23). The Opu transport systems also mediate the osmoregulated uptake of several other compatible solutes (4, 19, 25). For instance, proline betaine is taken up by *B. subtilis* via the OpuA and OpuC transporters (B. Kempf and E. Bremer, unpublished results).

OpuD is a secondary transporter that belongs to the betaine-choline-carnitine transporter family of uptake systems (22). In contrast, OpuA, OpuB, and OpuC are members of the *A*TP-*b*inding *c*assette (ABC) transporters, which use the energy released by ATP hydrolysis to transport substrates against a concentration gradient (16, 42). In general, ABC transporters are composed of four modules. The two nucleotide-binding domains and two transmembrane domains can be arranged in any possible combination. However, ABC import systems such as OpuA, OpuB, and OpuC contain a fifth module, a substrate-binding protein. This substrate-binding protein captures the substrate with high affinity and delivers it to the cognate transport system for subsequent ATP-dependent import. In gram-negative bacteria, binding proteins diffuse freely in the periplasmic space, while they are lipid anchored in the cytoplasmic membrane in gram-positive bacterial species, such as *B. subtilis* (1, 24, 26). However, it was recently shown that binding proteins can even be fused to the transmembrane domain of the ABC transporter (36, 43).

Despite this variation, all substrate-binding proteins from ABC transporters analyzed by X-ray crystallography today display a bilobal architecture. The ligand-binding site is located in a deep cleft situated between these two lobes, and residues located on both lobes usually contribute to substrate binding (45). Based on structural and kinetic investigations, a "Venus flytrap" mechanism was proposed to explain the ligand-binding mechanism on a molecular level (32, 39). Here, substrate-binding proteins undergo constant opening-closing motions in the absence of the ligand, and the amino acids connecting both domains act as a pivot point in such a hinge-bending motion. Upon ligand binding, the equilibrium between the open and closed states of the binding protein is shifted toward the so-called liganded/closed state, and the ligand is bound in a cleft located between both domains.

The ABC transporter OpuA from *B. subtilis* (19) has been analyzed functionally and structurally by in vivo or in vitro studies of either the whole transporter or its isolated components (17, 18, 20, 24, 26). The OpuA system consists of the cytoplasmic-membrane-associated ATPase OpuAA (18), the

* Corresponding author. Mailing address: Institute of Biochemistry, Heinrich Heine University Duesseldorf, Universitätsstr. 1, 40225 Düsseldorf, Germany. Phone: 49(0)211-81-10773. Fax: 49(0)211-81-15310. E-mail: lutz.schmitt@uni-duesseldorf.de.

‡ Both authors contributed equally to this work.

† Present address: Laboratory of Extreme Environments, Microbiology, University of West Brittany (Brest), European Institute of Marine studies, Technopôle Brest-Iroise, F-29280 Plouzané, France.

▽ Published ahead of print on 20 June 2008.

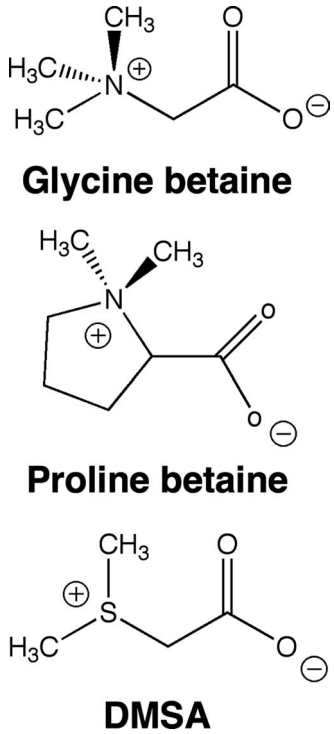

FIG. 1. Chemical structures of the OpuAC substrates used in this study.

integral membrane transport component OpuAB (17), and the extracellular ligand-binding protein OpuAC (24). The last protein is tethered to the cytoplasmic membrane via a lipid modification at its amino terminus (26). The crystal structure of OpuAC in complex with glycine betaine or proline betaine has been reported recently (20). The ligand-binding pocket of OpuAC is formed by three tryptophan residues arranged in a prism-like geometry suitable to coordinate the positive charge of the trimethylammonium group of glycine betaine or the dimethylammonium group of proline betaine by cation-π interactions. Additionally, hydrogen bonds with the carboxylate moiety of the ligand are formed. Structural differences between the OpuAC-glycine betaine and OpuAC-proline betaine complexes that allow a structural explanation for the drastic differences in affinity of OpuAC for these two ligands occur within the ligand-binding pocket. The dissociation constant (K_d) for the binding of glycine betaine by OpuAC is 17 $\pm$ 1 μM, whereas the K_d for the binding of proline betaine is 295 $\pm$ 27 μM (20).

Dimethylsulfonioacetate (DMSA), the closest sulfonium analog of glycine betaine (Fig. 1), is found as a secondary osmolyte in certain species of marine algae (6, 9). Previous studies have shown that DMSA (also referred to as sulfobetaine or dimethylthetin) (6) can function as an osmoprotectant for *Escherichia coli*, where it is accumulated via the ProP and ProU compatible-solute uptake systems (9). DMSA also serves as an osmoprotectant for *Pseudomonas aeruginosa* PAO1 (10) and the lactic acid bacterium *Tetragenococcus halophila* (2). Furthermore, DMSA is a substrate for the periplasmic binding protein from the glycine betaine and choline transporter OusB from *Erwinia chrysanthemi* (7). Interestingly, uptake of DMSA in *Sinorhizobium meliloti* is toxic and it becomes only osmoprotective in mutants that are unable to dimethylate this sulfobetaine (38).

To further analyze the principles of binding of compatible solutes to OpuAC, it is desirable to assess the importance of single tryptophans participating in the formation of the Trp prism and other amino acids contributing to ligand binding (20). Therefore, we have performed a mutational study of the ligand-binding site. Furthermore, we present the crystal structure of OpuAC in complex with the compatible solute DMSA, an efficient osmoprotectant for *B. subtilis* and a substrate of the OpuA transporter.

MATERIALS AND METHODS

Bacterial strains, plasmids, and culture conditions. The *E. coli* strains used in this study were maintained in Luria-Bertani medium (33) and were propagated at 37°C. For the selection of *E. coli* strains carrying derivatives of the expression vector pASK-IBA6 (IBA, Göttingen, Germany), ampicillin (100 μg ml^{-1}) was added to the liquid cultures and agar plates. Overproduction of the *B. subtilis* OpuAC protein and its mutant derivatives was carried out with the *E. coli* strain BL21 [F^- gal met[r] r$^-$ m$^-$ *hsdS*(λDE3)] (Stratagene, La Jolla, CA). For OpuAC overproduction, the plasmid-carrying BL21 strain was propagated in a defined minimal medium (MMA) (33) supplemented with 100 μg ampicillin ml^{-1}, 0.2% (wt/vol) Casamino Acids, and 0.5% (wt/vol) of glucose as the carbon source. Mutant derivatives of the *opuAC* expression plasmid pMH24 were recovered after transformation into Epicurian coli XL1-Blue {*recA1 endA1 gyrA96 thi-1 hsdR17 supE44 relA1 lac* [F′ *proAB lac1*^{q}*Z*ΔM15Tn*10*(Tet^r)]} (Stratagene, La Jolla, CA). The *B. subtilis* strains RMKB24 [Δ(*opuA*::*erm*)*4* Δ(*opuBD*::*tet*)*23 opuC-20*::Tn*10*(*spc*) Δ(*opuD*::*neo*)*2*] and RMKB34 [*opuA*$^+$ Δ(*opuBD*::*tet*)*23 opuC-20*::Tn*10*(*spc*) Δ(*opuD*::*neo*)*2*] are derivatives of the wild-type strain JH642 (*trpC pheA1*) (J. Hoch, Scripps Research Institute, CA). The genetic construction of these two *B. subtilis* mutants has been described by Kappes et al. (23).

B. subtilis strains were grown in Spizizen's minimal medium (SMM) with 0.5% (wt/vol) glucose as the carbon source and supplemented with L-tryptophan (20 μg ml^{-1}), L-phenylalanine (18 μg ml^{-1}), and a solution of trace elements (15). When required, the osmotic strength of SMM was increased by the addition of NaCl from a 5 M stock solution. For experiments that continuously monitored the growth of the *B. subtilis* cultures, 20 ml prewarmed SMM medium containing 1.2 M NaCl in a 100-ml Erlenmeyer flask was inoculated with a late-exponential-phase preculture grown in SMM with 0.4 M NaCl to an optical density at 578 nm (OD_{578}) of 0.1. These cultures were grown in a shaking water bath (set at 200 rpm) at 37°C. Compatible solutes (glycine betaine, proline betaine, and DMSA) were added to *B. subtilis* cultures to give a final concentration of 1 mM each, as required.

Chemicals. Glycine betaine was purchased from Sigma-Aldrich (Munich, Germany), proline betaine was obtained from Extrasynthèse (Genay Cedex, France), and DMSA was synthesized as described by Ferger and Vigneaud (13).

Overexpression and purification of the recombinant OpuAC protein in *E. coli*. Plasmid pMH24 is a *B. subtilis opuAC*$^+$ derivative of the expression vector pASK-IBA6 (IBA, Göttingen, Germany). In this recombinant plasmid, the *opuAC* coding region (without its own signal sequence and the codon specifying the amino-terminal cysteine residue of the mature OpuAC protein) (26) is positioned under the control of the anhydrotetracycline-inducible *tet* promoter present in the vector pASK-IBA6. This allows induction of transcription of the *opuAC* gene to high levels in the host strain BL21. The *opuAC* coding region has been inserted in pASK-IBA6 in-frame with an upstream *ompA* signal sequence and the codons for a Strep-TagII affinity peptide. This allowed the secretion of the Strep-TagII-OpuAC fusion protein into the periplasm of *E. coli*, from which it could be released by cold osmotic shock and recovered by affinity chromatography on Strep-Tactin Sepharose (IBA, Göttingen, Germany). Strain BL21(pMH24) grown in 5 liters of defined MMA to an OD_{578} of 0.1 was inoculated from an overnight culture of BL21(pMH24) prepared in the same medium. *opuAC* transcription was induced at an OD_{578} of 0.7 of the culture by the addition of 0.2 μg ml^{-1} anhydrotetracycline. Growth of the culture of BL21(pMH24) was then continued for 1.5 h at 37°C with avid stirring. Subsequently, cells were harvested by centrifugation (10 min, 3,000 $\times$ *g*). To release periplasmic proteins from the BL21(pMH24) cells, the cell pellet was resuspended in 50 ml of ice-cold buffer P (50 mM Tris-HCl, pH 8.0, 100 mM NaCl, 500 mM sucrose) and incubated for 30 min on ice. Soluble periplasmic proteins

were isolated by two subsequent centrifugation steps. First, the supernatant was centrifuged for 15 min at 21,000 × *g* to remove cellular debris. Subsequently, the supernatant was recentrifuged for 60 min at 120,000 × *g* to remove denatured proteins. The cleared, soluble periplasmic protein fraction was then loaded onto a 10-ml Strep-Tactin column (IBA, Göttingen, Germany) preequilibrated with 10 bed volumes of buffer W (50 mM Tris-HCl, 100 mM NaCl, pH 8.0). After the column was washed with 10 bed volumes of buffer W, bound proteins were eluted from the affinity resin with buffer E (50 mM Tris-HCl, pH 8.0, 100 mM NaCl, 2.5 mM desthiobiotin). OpuAC-containing fractions were collected in 5-ml portions.

Two forms of the recombinantly produced OpuAC were released from the periplasmic fraction: (i) the nonprocessed OmpA-Strep-TagII-OpuAC fusion and (ii) the processed Strep-TagII-OpuAC form. To remove the OmpA signal sequence and Strep-TagII from unprocessed OmpA-Strep-TagII-OpuAC and Strep-TagII from processed Strep-TagII-OpuAC, OpuAC-containing fractions were pooled and incubated overnight at 23°C with 0.5 U factor Xa (Novagen, Darmstadt, Germany) per 10 μg of OpuAC in buffer E in the presence of 4 mM $CaCl_2$. Complete removal of the OmpA signal sequence and Strep-TagII from OpuAC was verified by sodium dodecyl sulfate-polyacrylamide gel electrophoresis. OpuAC was concentrated to a volume of approximately 500 μl by using Vivaspin 4 (Vivascience, Hannover, Germany) concentrator columns (exclusion size, 10 kDa). Subsequently, the protein was passed through a HiTrapQ anion exchange column (GE Healthcare, Munich, Germany) to remove factor Xa from the protein preparation. The column was washed with a buffer containing 25 mM Tris-HCl and 25 mM NaCl (pH 8.3). OpuAC does not bind to the HiTrapQ material and passes through the column, whereas factor Xa bound to the HiTrapQ material. Finally, isolated OpuAC was dialyzed twice against 5-liter volumes of 10 mM Tris-HCl (pH 7.0) at 4°C overnight and stored at 4°C until further use. In general, approximately 1.5 mg of pure OpuAC protein was obtained per liter of *E. coli* culture. The functionality of the purified OpuAC protein was assessed by fluorescence spectroscopy, using changes in the intrinsic tryptophan fluorescence of OpuAC upon substrate binding (e.g., glycine betaine), as detailed by Horn et al. (20). Protein concentrations were estimated based on the theoretical molar extinction coefficient of OpuAC, yielding the following correlation: an A_{280} of 1.0 corresponds to 0.5 mg ml^{-1} OpuAC. OpuAC used for crystallization experiments was concentrated to approximately 10 mg ml^{-1} by using Vivaspin 4 (Vivascience, Hannover, Germany) concentrator columns (exclusion size, 10 kDa).

Site-directed mutagenesis of the *opuAC* gene. To determine the individual contribution of the amino acids forming the Trp prism (Trp^{72}, Trp^{178}, and Trp^{225}) and His^{230} to the stability of the OpuAC-glycine betaine, OpuAC-proline betaine, and OpuAC-DMSA complexes (20), the corresponding codons in the *opuAC* gene were changed via site-directed mutagenesis, using a QuikChange site-directed-mutagenesis kit (Stratagene, La Jolla, CA) and custom-synthesized mutagenic primers (Biomers, Ulm, Germany). These experiments were conducted with the $opuAC^+$ plasmid pMH24. The entire coding region of the mutant *opuAC* genes was sequenced to ensure the presence of the desired mutation and the absence of undesired alterations in the *opuAC* coding region. Double and triple mutants were generated from the plasmids bearing the corresponding single or double mutations at the desired positions. The following mutant *opuAC* variants were generated on plasmid pMH24: pMH26 (Trp72→Ala [TGG→GCG]), pMH27 (Trp72→Phe [TGG→TTT]), pMH28 (Trp72→Tyr [TGG→TAT]), pMH29 (Trp178→Ala [TGG→GCG]), pMH30 (Trp178→Phe [TGG→TTT]), pMH31 (Trp178→Tyr [TGG→TAT]), pMH32 (Trp225→Ala [TGG→GCG]), pMH33 (Trp225→Phe [TGG→TTT]), pMH34 (Trp225→Tyr [TGG→TAT]), pMH35 (His230→Ala [CAT→GCG]), pMH36 (Trp72→Phe, Trp178→Phe [TGG→TTT]), pMH37 (Trp72→Tyr, Trp178→Tyr [TGG→TAT]), pMH38 (Trp72→Phe, Trp178→Phe, Trp225→Phe [TGG→TTT]), pMH39 (Trp72→Tyr, Trp178→Tyr, Trp225→Tyr [TGG→TAT]), pML1 (Trp72→Phe, Trp225→Phe [TGG→TTT]), and pML2 (Trp72→Tyr, Trp225→Tyr [TGG→TAT]). The mutant *opuAC* genes were overexpressed in strain BL21 as described above for the wild-type *opuAC* gene. Mutant OpuAC proteins were then purified exactly as described for wild-type OpuAC. The mutant proteins were recovered with yields similar to those of the wild type, indicating that the introduced mutations in *opuAC* did not alter the stability of the mutant proteins.

Determination of the dissociation constants of the OpuAC–compatible-solute complexes. The dissociation affinity of the OpuAC-glycine betaine, proline betaine, or DMSA complex was determined as described by Horn et al. (20). In brief, the intrinsic tryptophan fluorescence of OpuAC was monitored from 300 nm to 450 nm by using a Cary Eclipse fluorescence spectrometer (Varian, Surrey, United Kingdom). The excitation wavelength was set to 295 nm, the slit width was 5 nm, and the temperature was maintained at room temperature (22 ± 1°C) by using a circulating water bath. Different amounts of the substrates were titrated to 1-ml OpuAC samples (250 nM in 10 mM Tris-HCl, pH 7.0), and fluorescence was measured after equilibration (5 min). Changes in the maximum emission wavelength (glycine betaine or proline betaine), determined by an automated peak search routine, or changes in the fluorescence intensity (DMSA) were plotted against substrate concentration after background correction. Upon binding of glycine betaine or proline betaine to OpuAC, a blue shift of $\lambda_{em,max}$ from 345 nm in the absence of ligand to 336 nm under substrate saturation conditions was observed. The changes of the emission maxima or fluorescence intensity due to the concentration of bound substrates could by analyzed using a 1:1 binding site model employing equation 1 (glycine betaine and proline betaine) or equation 2 (DMSA):

$$\lambda_{em,max} = \lambda_{em,max0} + [\Delta\lambda_{em,max} \times [S_0]/([S_0] + K_d)] \quad (1)$$

Here, $\lambda_{em,max}$ is the emission wavelength maximum for a given substrate concentration, $\lambda_{em,max0}$ is the emission wavelength maximum without the substrate, $\Delta\lambda_{em,max}$ is the maximal emission wavelength maximum shift, and $[S_0]$ is the substrate concentration.

$$F = F_0 + [\Delta F \times [S_0]/([S_0] + K_d)] \quad (2)$$

Here, F is the fluorescence intensity for a given substrate concentration, F_0 is the fluorescence intensity without the substrate, ΔF is the maximal change in fluorescence intensity, and $[S_0]$ is the substrate concentration. All K_d measurements of OpuAC and its mutant derivatives that are summarized in Table 1 represent the averages of results for at least three independent measurements, with standard deviations given as errors.

Crystallization of the OpuAC-DMSA complex, data collection, and model refinement. Crystals of the OpuAC-DMSA complex were obtained under conditions similar to the ones described for the glycine betaine and proline betaine complexes (20). Prior to crystallization, OpuAC (at a concentration of 10 mg ml^{-1}) was incubated with 3 mM DMSA. Subsequently, 1 μl of protein solution was mixed with 1 μl of reservoir solution and 0.5 μl of 100 mM L-cysteine. The reservoir solution contained 100 mM Tris-HCl (pH 8.25), 150 mM NH_4 acetate, and 15% (wt/vol) PEG 4000. Crystal plates appeared at room temperature after several weeks, with final dimensions of 200 μm by 100 μm by 30 μm. Crystals were transferred into cryo buffer (150 mM Tris-HCl [pH 8.3], 20% [wt/vol] ethylene glycol, 200 mM NH_4 acetate, 20% [wt/vol] PEG 4000) and flash frozen in liquid nitrogen. Diffraction data were collected at 100 K at EMBL beam line BW-7A at DESY, Hamburg, Germany. Data were indexed and scaled with XDS and further analyzed using the CCP4 program package (8). The structure was solved by molecular replacement using AMoRe (35), with the OpuAC-glycine betaine monomer (20) as search model. Four monomers were found in the asymmetric unit, and the initial structure was further improved by manual rebuilding in $2F_o$-F_c and $1F_o$-F_c electron density maps by using Coot (12) and subsequent rounds of refinement employing REFMAC5 (34). During the initial refinement cycles, strict NCS restrains (27) were maintained, which were released in the last five cycles of refinement. The quality of the model was verified with the MolProbity server (http://molprobity.biochem.duke.edu/) and is summarized in Table 2. The R_F and R_{free} values are 28.5% and 36.4%, respectively. However, at the higher end of the range expected at this resolution (28), they are still within the limits, and the quality of the electron density map allowed a detailed analysis of the structure.

Protein Data Bank accession number. The coordinates of the OpuAC-DMSA complex have been deposited in the RCSB Protein Data Bank under accession code 3CHG.

RESULTS AND DISCUSSION

DMSA is a substrate for the OpuA transporter and confers osmoprotection in *B. subtilis*. Previous growth studies and transport assays have shown that DMSA is also an effective osmoprotectant for *B. subtilis* and is acquired by the cell via the OpuA, OpuC, and OpuD osmolyte transport systems (G. Nau-Wagner, M. Jebbar, and E. Bremer, unpublished results). Hence, glycine betaine (22–24) and its sulfur analog DMSA are taken up via the same three transport systems. We analyzed the uptake of DMSA via the OpuA transporter by growth experiments. Both glycine betaine and DMSA (provided at concentrations of 1 mM each) were very effective osmoprotectants in strain RMKB34, which has $OpuA^+$ but is defective in the compatible-solute uptake systems OpuB, OpuC, and

TABLE 1. Dissociation constants of glycine betaine, proline betaine and DMSA to the wild type OpuAC protein and its mutant derivatives[a]

Amino acid(s)	Mutated residue	Dissociation constant of:		
		Glycine betaine	Proline betaine	DMSA
Wild type		22 ± 4 μM	267 ± 6 μM	102 ± 11 μM
Trp^{72}	A	≫5 mM	≫5 mM	≫5 mM
	F	1.4 ± 0.4 mM	≫5 mM	≫5 mM
	Y	750 ± 8 μM	≫5 mM	≫5 mM
Trp^{178}	A	≫5 mM	≫5 mM	≫5 mM
	F	14 ± 1.4 μM	243 ± 28 μM	56 ± 17 μM
	Y	548 ± 263 μM	58 ± 27 μM	≫5 mM
Trp^{225}	A	≫5 mM	≫5 mM	≫5 mM
	F	308 ± 18 μM	1.93 ± 0.03 mM	≫5 mM
	Y	67 ± 22 μM	1.25 ± 0.28 mM	425 ± 30 μM
His^{230}	A	392 ± 92 μM	491 ± 195 μM	259 ± 55 μM
$Trp^{72/178}$	F	≫5 mM	≫5 mM	≫5 mM
	Y	≫5 mM	≫5 mM	≫5 mM
$Trp^{72/225}$	F	≫5 mM	≫5 mM	≫5 mM
	Y	≫5 mM	≫5 mM	≫5 mM
$Trp^{72/178/225}$	F	≫5 mM	≫5 mM	≫5 mM
	Y	≫5 mM	≫5 mM	≫5 mM

[a] By use of a fluorescence-based assay, the dissociation constants of glycine betaine, proline betaine, and DMSA were determined for the wild-type protein and each of the generated OpuAC variants. Reported K_d values are the averages of results for at least three independent experiments, with the standard deviation reported as the error. ≫5 mM indicates that no binding of ligand was detected up to the highest concentration employed in the assay (5 mM). In the case of low-affinity binders, such as W72F or W178Y, the final substrate concentration was two- to threefold higher than the K_d value. Abbreviations: A, alanine; F, phenylalanine; Y, tyrosine.

OpuD (Fig. 2A). When the OpuA system is inactivated by a gene disruption mutation in an otherwise $OpuB^-$, $OpuC^-$, and $OpuD^-$ background (RMKB24), osmoprotection by glycine betaine is completely blocked, as has been reported previously by Kappes et al. (22), and osmoprotection by DMSA is greatly reduced (Fig. 2B). We conclude from these growth experiments that DMSA is a substrate for the OpuA transporter but that a fourth uptake route for DMSA that remains to be identified seems to operate in *B. subtilis*. Since DMSA can enter the cell via the OpuA system, this sulfobetaine should be recognized by the ligand-binding protein (OpuAC) of the OpuA transporter.

DMSA is bound by the purified *B. subtilis* OpuAC protein. We overexpressed the *B. subtilis opuAC* gene in *E. coli* and purified the recombinant OpuAC protein by affinity chromatography to homogeneity (data not shown). To determine the affinities of glycine betaine, proline betaine, and DMSA for the purified OpuAC protein, an intrinsic Trp fluorescence-based binding assay was employed. A spectrum and the corresponding binding curve for DMSA are shown in Fig. 3. Binding of glycine betaine and proline betaine to OpuAC resulted in a blue shift of the emission spectra of 9 nm (glycine betaine; data not shown) and 6 nm (proline betaine; data not shown), respectively. This shift in emission maximum was subsequently used to determine the dissociation constants of the complexes according to equation 1 (see Materials and Methods). A 1:1 binding isotherm described the experimental data adequately, and K_d values could be calculated to 22 ± 4 μM and to 267 ± 6 μM for glycine betaine and proline betaine, respectively (Table 1). These values are in very good agreement with those previously determined for these two OpuAC substrates (for glycine betaine, K_d = 17 ± 1 μM, and for proline betaine, K_d = 295 ± 27 μM) by Horn et al. (20). In contrast to the binding of glycine betaine and proline betaine to OpuAC, binding of DMSA to OpuAC induced only a marginal blue shift of the emission maximum (2 nm; data not shown). Therefore, the decrease in fluorescence intensity was used to determine the binding constant according to equation 2 (see Materials and Methods), assuming again a 1:1 binding isotherm (Fig. 3B). Here, a calculated K_d value of 102 ± 11 μM was determined, an affinity that is between the values determined for the other two OpuAC ligands (Table 1). From a chemical point of view, the structures of the individual ligands (Fig. 1) do not provide any ready explanation for these differences in affinity. All three ligands contain a carboxylate moiety and a delocalized positive charge. Since the K_d value of DMSA is in between the ones for glycine betaine and proline betaine, the nature of the delocalized positive charge does not seem to be relevant for the apparent affinity differences (Table 1).

Crystal structure of OpuAC with its ligand DMSA. To gain insight into the molecular determinants that govern binding of DMSA by OpuAC, we crystallized this ligand-binding protein in the presence of DMSA and determined the crystal structure of the OpuAC-DMSA complex at a resolution of 2.8 Å. The structure was solved by molecular replacement, using the recently determined OpuAC-glycine betaine structure (20) as a search model, and refined using REFMAC5 (34). A summary of the data collection statistics and refinement details as well as the model content are given in Table 2. As expected, the overall fold of OpuAC in complex with DMSA (RCSB Protein

TABLE 2. Data collection and refinement statistics for the OpuAC-DMSA complex

Crystal parameter at 100 K[a]	Value(s)
Space group	$P2_1$
Unit cell parameters	
a, *b*, *c* (Å)	56.51, 150.61, 58.96
α, β, γ (deg)	90.0, 104.54, 90.0
Data collection and processing	
Wavelength (Å)	0.98
Resolution (Å)	20–2.8 (2.85–2.8)
Mean redundancy	2.4
Unique reflections	24,818
Mosaicity (°)	0.4
Completeness (%)	93.0 (96.5)
I/σ	6.8 (3.0)
R_{merge}[b]	16.4 (28.8)
Refinement	
R_F[c] (%)	28.5
R_{free}[d] (%)	36.4
Overall B factor from Wilson scaling (Å^2)	27.4
RMSD from ideal	
Bond lengths (Å)	0.07
Bond angles (deg)	1.12
Average B factors (Å^2)	27.85
Ramachandran plot	
Most favored (%)	89.2
Allowed (%)	9.9
Generously allowed (%)	
Disallowed (%)	0.9
Model content	
Monomers/ASU	4
Protein residues	20–272
Ligand	Four DMSA

[a] Crystal parameters and data collection statistics are derived from SCALEPACK (37). Refinement statistics were obtained from REFMAC5 (34), and Ramachandran analysis was performed using MolProbity. Data in parentheses correspond to the highest resolution shell (2.85 to 2.80 Å). RMSD, root mean square deviation.

[b] R_{sym} is defined as $\sum_{hkl}\sum_i[I_i(hkl) - \langle I(hkl)\rangle]/\sum_{hkl}\sum_i I_i(hkl)$.

[c] R_F is calculated as $\sum_{hkl}[(F_{obs}) - (F_{calc})]/\sum_{hkl}(F_{obs})$.

[d] R_{free} is calculated as R_F but for 5% randomly chosen reflections that were omitted from all refinement steps. All amino acids located in the disallowed region of the Ramachandran plot (0.9%, or 9 residues) are involved in crystal contacts.

Data Bank accession code 3CHG) is similar to that of the recently published OpuAC complexes containing either glycine betaine (RCSB Protein Data Bank accession code 2B4L) or proline betaine (RCSB Protein Data Bank accession code 2B4M) (20). The OpuAC-DMSA complex exhibits the characteristic bilobal protein fold observed for many binding proteins of prokaryotic ABC transport systems (32, 39, 45).

The quality of the initial electron density map of the OpuAC protein with the bound DMSA allowed an unambiguous placement of the ligand and thereby the localization of the sulfonium moiety of DMSA despite the medium resolution (2.8 Å) of the overall OpuAC-DMSA structure. In contrast to the structure of the OpuAC-glycine betaine complex (20), the asymmetric unit of the OpuAC-DMSA crystal structure contained four protomers. Since the root mean square deviation of the individual protomers in the asymmetric unit was smaller than 1 Å, the description of the structure will be restricted to a single protomer (monomer D). Two of these protomers are related via noncrystallographic symmetry, which was used during the initial steps of structure refinement but released in the last cycles of refinement. As shown in Fig. 4, the overall architecture of the DMSA binding site was identical to that for the OpuAC-glycine betaine complex (20) and is composed of three tryptophans (Trp^{72}, Trp^{178}, and Trp^{225}) and one histidine (His^{230}). Additionally, the carboxylate of DMSA interacts with the backbone amides of Gly^{26} and Ile^{27} via hydrogen bonds (3.5 Å and 2.9 Å, respectively), as has been previously observed in both the OpuAC-glycine betaine and the OpuAC-proline betaine complexes (20). These two hydrogen bonds, together with the interaction of DMSA with His^{230} (distance of 3.2 Å), fix the carboxylate moiety of DMSA within the ligand-binding site (Fig. 4). The dimethylsulfonium group of DMSA interacts with the individual tryptophans of the Trp prism (Trp^{72} Trp^{178} Trp^{225}) (20) via cation-π interactions (31). All distances range between 3.5 and 4.0 Å, perfectly fitting the van der Waals interactions and fulfilling the requirements of cation-π interactions (30). However, a closer inspection reveals that only 19 cation-π interactions and 6 van der Waals interactions are present in the DMSA complex, while 22 cation-π interactions were determined for the OpuAC-glycine betaine complex (20). In contrast, only 6 cation-π and 15 van der Waals interactions are found in the OpuAC-proline betaine complex (13). More important, however, is the fact that the interaction distances between His^{230} and the ligands glycine betaine, DMSA, and proline betaine are 2.6 Å, 3.5 Å, and 4.7 Å, respectively. The distance of His^{230} to proline betaine is even beyond the effec-

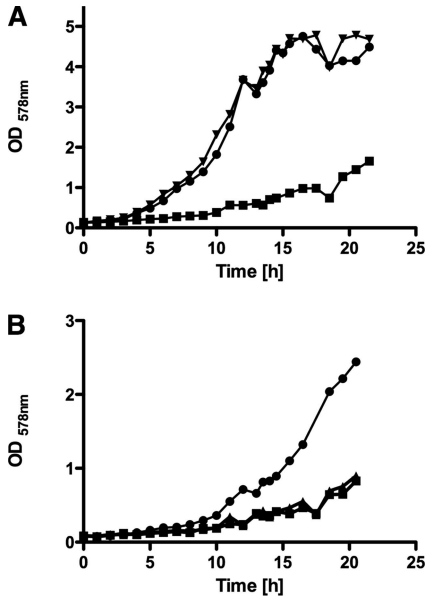

FIG. 2. Osmoprotective effects of the compatible solutes glycine betaine and DMSA for *B. subtilis*. (A) The $OpuA^+$ ($OpuB^-$ $OpuC^-$ $OpuD^-$) strain RMKB34 was grown in SMM with 1.2 M NaCl (■), 1.2 M NaCl with 1 mM glycine betaine (●), and 1.2 M NaCl with 1 mM DMSA (▲). (B) The $OpuA^-$ ($OpuB^-$ $OpuC^-$ $OpuD^-$) strain RMKB24 was grown in SMM with 1.2 M NaCl (■), 1.2 M NaCl with 1 mM glycine betaine (▲), and 1.2 M NaCl with 1 mM DMSA (●). Cultures (20 ml) were inoculated to an OD_{578} of 0.1 from overnight cultures pregrown in SMM with 0.4 M NaCl and were propagated in 100-ml Erlenmeyer flasks in a shaking water bath (220 rpm) at 37°C. Cell growth was monitored over time by measuring the OD_{578}.

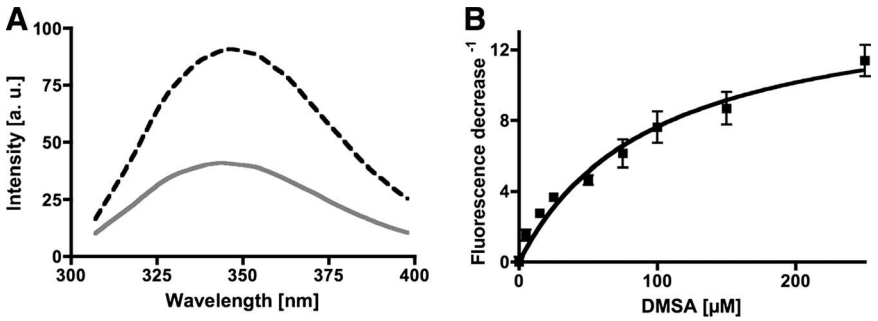

FIG. 3. Ligand binding of OpuAC with DMSA. (A) Emission spectra of the protein in the absence (solid line) or presence (dashed line) of 1 mM substrate. (B) Equilibrium binding titration experiments with DMSA. a.u., arbitrary units.

tive distance of a salt bridge. Horn et al. (20) used this distance argument to explain the drastically low affinity of OpuAC for proline betaine (K_d = 295 ± 27 μM) compared to the affinity of OpuAC for glycine betaine (K_d = 17 ± 1 μM). In light of the OpuAC-DMSA structure reported here and the previously reported analysis of the OpuAC-glycine betaine and OpuAC-proline betaine complexes (20), the combinations of different numbers of cation-π and van der Waals interactions contribute significantly to ligand binding. Furthermore, the presence (in the case of glycine betaine and DMSA) or the absence (in the case of proline betaine) of an interaction between the ligand and His^{230} also appears important for substrate binding.

To compare the positioning of the three OpuAC substrates within the ligand-binding sites, we superimposed the OpuAC-glycine betaine, OpuAC-proline betaine, and OpuAC-DMSA crystal structures. As shown in Fig. 5, the ligand-binding site of the OpuAC-DMSA complex almost perfectly matches those of the OpuAC-glycine betaine and the OpuAC-proline betaine structures. Next to the slightly different conformations of His^{230} in the three structures (Fig. 5), the most important difference between the OpuAC structures is the conformation of the indole moiety of Trp^{178}. In the OpuAC-proline betaine complex, it is flipped nearly 180° with respect to the positions in the OpuAC-DMSA and the OpuAC-glycine betaine complexes. Thus, it is tempting to speculate that the orientation of this side chain might contribute to the overall affinity of OpuAC for either its high (glycine betaine)-, its medium (DMSA)-, or its low (proline betaine)-affinity ligands.

Site-directed mutagenesis of the OpuAC ligand-binding pocket. The analysis of the three OpuAC structures in complex with the various ligands provides a molecular framework for describing the interactions and affinities of different compatible solutes for OpuAC. To analyze the contribution of individual amino acid residues within the OpuAC binding pocket to ligand binding, we performed a site-directed mutagenesis study. We mutagenized the *opuAC*$^+$ overexpression plasmid pMH24 by using the QuikChange site-directed-mutagenesis kit (Stratagene) and a set of mutagenic DNA primers. In total, we generated 16 *opuAC* mutants (see Materials and Methods). Each of these mutant *opuAC* genes were overexpressed in

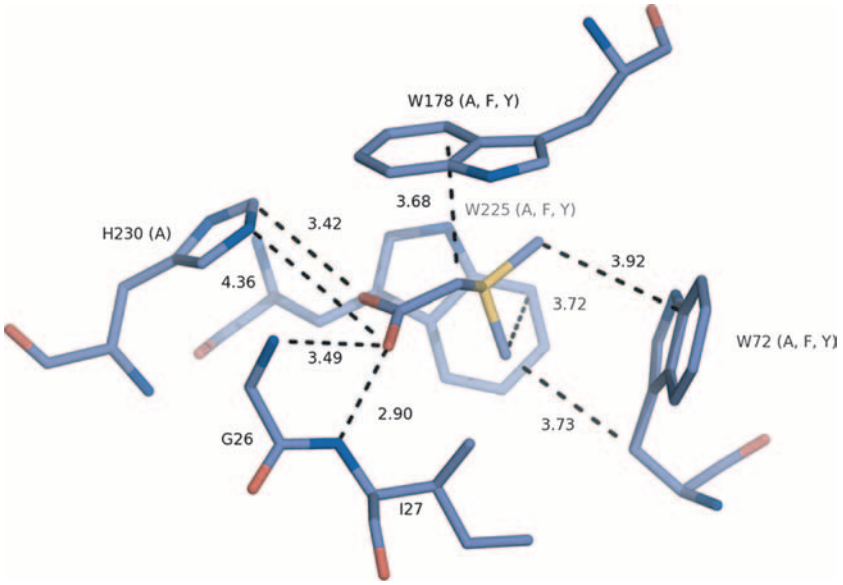

FIG. 4. View of the ligand-binding pocket of the OpuAC-DMSA complex. Interactions between the OpuAC protein and its ligand DMSA are highlighted by dashed lines. Highlighted are the three tryptophans (Trp^{72}, Trp^{178}, and Trp^{225}) and the histidine residue (His^{230}), which constitute the binding pocket. Amino acids given in single-letter code in parentheses indicate the mutations performed in this study.

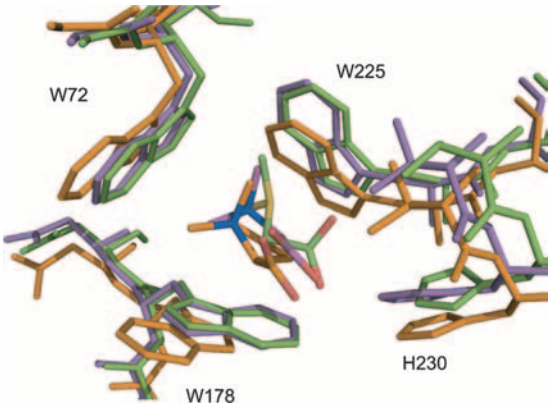

FIG. 5. View of the superpositioning of the ligand-binding sites of the OpuAC-glycine betaine, OpuAC-proline betaine, and OpuAC-DMSA complexes. Residues involved in glycine betaine coordination are shown in green, residues involved in proline betaine binding are shown in orange, and residues involved in DMSA binding are shown in purple. For simplicity, the backbone contacts of the ligands with Gly^{26} and Ile^{27} have been omitted from the representation.

strain BL21, and the variant OpuAC proteins were purified to homogeneity by affinity chromatography. The purified mutant OpuAC proteins were analyzed for binding to and affinity for glycine betaine, proline betaine, and DMSA by using fluorescence spectroscopy, and these data are summarized in Table 1. For a structural summary, see Fig. 4.

The generated mutations can be principally subdivided into four classes. (i) The three tryptophan residues forming the Trp prism (Trp^{72}, Trp^{178}, and Trp^{225}) were mutated individually to alanine residues. (ii) The three Trp residues were separately mutated to either phenylalanine or tyrosine residues. (iii) We also simultaneously changed the three tryptophan residues forming the Trp prism to either Phe or Tyr. (iv) His^{230} was changed to alanine.

To determine the influence of Trp residues within the OpuAC binding site on complex stability, we assessed individual Ala substitutions for substrate binding. As shown in Table 1, mutation of any of the three tryptophans to alanine resulted in a complete loss of ligand binding. This is different from the situation found in the glycine betaine/proline betaine binding protein ProX from *E. coli*. Here, three Trp residues, arranged in a box-like structure, constitute the binding surface for the trimethlyammonium head group of glycine betaine and the dimethylammonium head group of proline betaine via cation-π interactions (40). Two of these Trp residues (Trp^{65} and Trp^{140}) can be changed to Ala residues with modest effects on substrate binding. However, the replacement of Trp^{188} with Ala results in a complete loss of binding of glycine betaine (40). Consequently, in the box-like arrangement of the Trp residues found within the binding site of ProX, only a single Trp residue is critical for substrate binding. The other two Trp residues appear to stabilize the substrate within the ligand-binding pocket (33).

As elaborated by Dougherty and coworkers (11, 31), the strength of a cation-π interaction between a ligand and a protein decreases from Trp to Tyr to Phe, thus following the decrease in electronegative potential for the indole, phenole, and benzole side chains of the amino acids. We therefore individually changed Trp^{72}, Trp^{178} and Trp^{225} of OpuAC to either Phe or Tyr residues. Exchange of a single tryptophan for either Phe or Tyr resulted in a complex response with respect to ligand binding, and this was dependent on the tryptophan mutated and the ligand analyzed (Table 1). These substitutions in general caused substantial decreases in affinity of OpuAC for its three ligands, and in several cases, no substrate binding could be detected at all (Table 1). This result is surprising, since the site-directed change of the Trp residues to either Phe or Tyr residues within the *E. coli* ProX ligand-binding site has essentially no influence on ligand binding (40). Furthermore, mutational analysis of the aromatic residues within the binding site of the ectoine/hydroxyectoine binding protein EhuB from *Sinorhizobium meliloti* (14, 21) revealed that the strength of the cation-π interaction is of key importance for the efficiency of substrate binding. An aromatic box composed of Phe^{24}, Tyr^{60}, and Phe^{80} forms a central part of the ligand-binding site of the EhuB protein, allowing substrate binding with K_d values in a low-micromolar range (14). Replacements of these aromatic residues by Trp, the amino acid that has the strongest electronegative potential and is hence best suited for cation-π interactions (11, 31), created superbinding variants of EhuB that bind both ectoine and hydroxyectoine with K_d values in a low nM range (14).

Simultaneous change of either two tryptophans ($Trp^{72/178}$, $Trp^{72/225}$, or $Trp^{178/225}$) or all three tryptophans to either Phe or Tyr residues completely abolished ligand binding (Table 1). This clearly demonstrates that a single Trp residue paired with two other aromatic amino acids is not sufficient for OpuAC to bind any of the three substrates tested. We are thus tempted to speculate that the Trp prism found in OpuAC has been evolutionarily optimized for ligand binding in such a way that only minor variations are permitted. This argument is strengthened by our database searches. We aligned the amino acid sequences of 64 OpuAC related proteins (Fig. 6) and found that Trp^{72}, Trp^{178}, and Trp^{225} are completely conserved, regardless whether the proteins align directly with OpuAC, whether the alignment requires the inversion of N- and C-terminal domains (20), or whether the ligand-binding portion is fused to the transmembrane domain of the corresponding ABC transport systems (Fig. 6, with further details provided in the legend).

A rather surprising result is obtained when Trp^{178} is changed to Tyr. This substitution causes a drastic decrease in glycine betaine binding and abolishes DMSA binding but substantially increases the binding of proline betaine. Currently, we have no biochemical or structural explanation for these findings.

The analysis of the crystal structures of the OpuAC-glycine betaine and OpuAC-proline betaine complexes suggested that an additional hydrogen bond between the carboxylate of glycine betaine and His^{230} was responsible for the 17-fold higher affinity of OpuAC for glycine betaine than for proline betaine (20). In a His^{230}-to-Ala substitution, this critical hydrogen bond will be abolished, thus predicting that the binding affinity of OpuAC for glycine betaine should be strongly decreased and should approach that of proline betaine. The data summarized in Table 1 demonstrate that this is indeed the case and thus support the prediction made by Horn et al. (20) based on the interpretation of the OpuAC structures. Since His^{230} also makes contacts to the carboxylate of DMSA, binding of the sulfobetaine is also substantially reduced by the replacement of

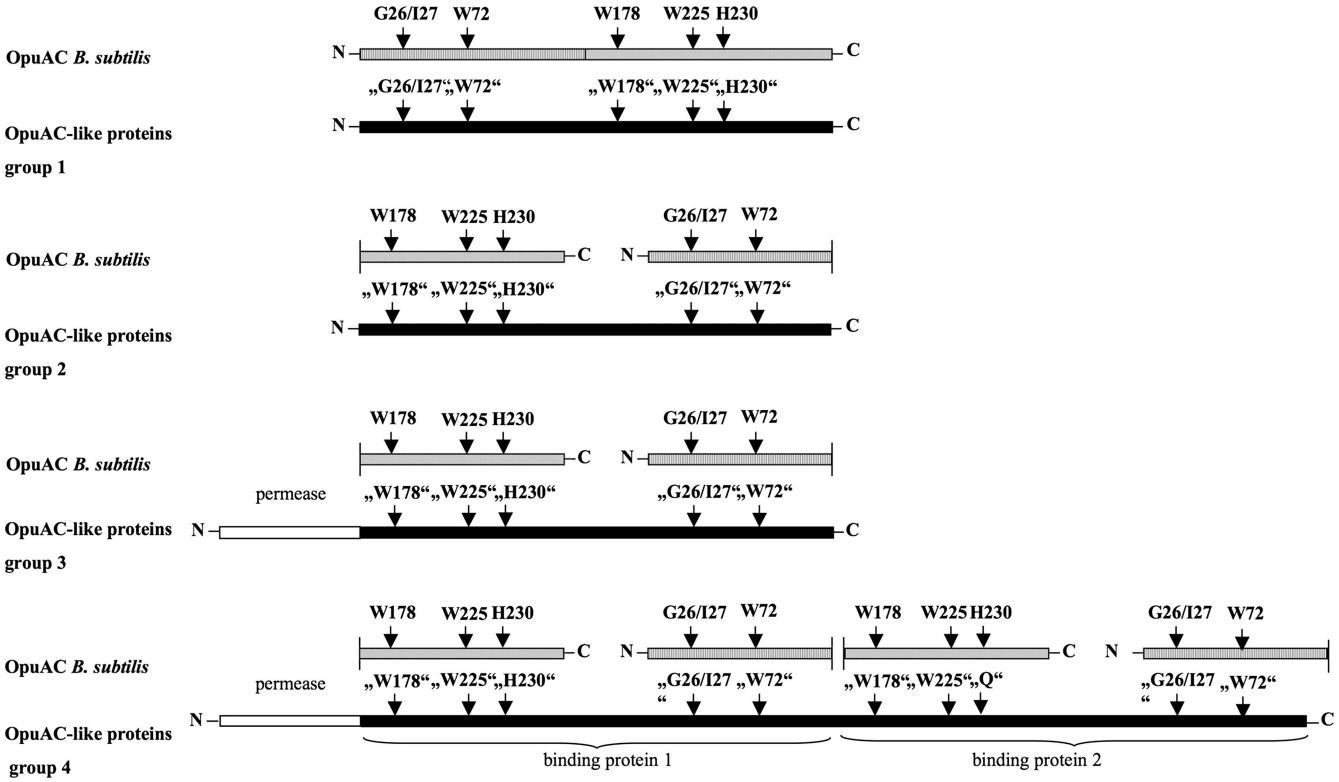

FIG. 6. Domain organization of glycine betaine binding proteins related to OpuAC from *B. subtilis*. Data base searches using the BLAST program showed that there are four classes of ligand-binding proteins that are related to OpuAC from *B. subtilis*. The OpuAC protein from *B. subtilis* is shown with the residues involved in binding of the trimethylammonium head group of glycine betaine (W72, W178, W225) and the carboxylate of glycine betaine (G26, I27, H230). Group 1 contains those proteins that align directly with the OpuAC protein. An example is the glycine betaine binding protein GbuC from *Listeria monocytogenes* (29). Group 2 is composed of proteins that align with the OpuAC protein when the N- and C-terminal domains are inverted. An example is the glycine betaine binding protein OtaC from the archaeon *Methanosarcina mazei* (41). Binding protein domains that are fused to the transmembrane domain of the ABC transport system and contain the domain inversion form group 3. An example is the glycine betaine binding/transmembrane protein OpuBC (also referred to as BusAB) from *Lactococcus lactis* (36, 44). Finally, group 4 of the OpuAC related proteins contain those examples where the transmembrane domain is fused to a duplicated binding protein domain both of which contain the domain inversion. This type of fusion protein was first noticed by van der Heide and Poolman (43). An example of this group of OpuAC-related proteins is present in *Streptomyces coelicolor* (NP_625895). But in contrast to the other mentioned glycine betaine binding proteins, the substrate specificity of this fused binding protein has not been experimentally assessed. For the various alignments, the N-terminal and C-terminal domains of OpuAC were split between the amino acids 168/169 as initially described by Horn et al. (20).

His^{230} with Ala (Table 1). These findings are consistent with the view that interactions between the carboxylate of the ligands and His^{230} make important contributions to the overall affinity of the OpuAC protein for its ligands. Thus, His^{230} has a prime role in modulating affinity of the OpuAC–compatible-solute complexes. Although not as completely conserved as the three tryptophan residues forming the Trp prism of OpuAC, changes of His^{230} in OpuAC-related proteins occur only by amino acids that are capable of forming salt bridges or hydrogen bonds (20).

Conclusions. Site-directed mutagenesis of compatible-solute-binding proteins (references 14 and 40 and this study) has demonstrated that individual amino acids within the aromatic scaffold make different contributions to ligand binding. Furthermore, the strength of the cation-π interaction is a key factor for the efficiency of ligand binding (14). In addition to cation-π interactions, interactions between the carboxylate of the substrates and the ligand-binding protein permit the precise positioning of the compatible solute within the binding site. As shown in this study, loss of the interaction between His^{230} of OpuAC and the carboxylate of glycine betaine or DMSA results in a substantial drop of affinity (Table 1). Thus, the correct positioning of the ligand within the binding cavity requires molecular interactions involving both the positively charged head group and the negatively charged carboxylic tail of these organic solutes. Therefore, a limited set of molecular interactions is used in various compatible-solute-binding proteins to precisely position the ligand within the binding site and a modulation of the interplay between these interactions generates different hierarchies in substrate affinity.

ACKNOWLEDGMENTS

We are indebted to Matthew Groves for his excellent support during data acquisition at beam line BW-7B, EMBL Outstation Hamburg. M.H. is a recipient of a Ph.D. fellowship from the International Max-Planck Research School (Marburg, Germany).

This work was supported by the Fonds der chemischen Industrie (to E.B.), the Deutsche Forschungsgemeinschaft (SFB 395 to E.B.), the Max-Planck Institut für terrestrische Mikrobiologie (Marburg, Germany) (to E.B.), and grants from the Heinrich Heine University Düsseldorf (to L.S.).

REFERENCES

1. **Ames, G. F.-L.** 1992. Bacterial periplasmatic permeases as model systems for the superfamily of traffic ATPases, including the multidrug resistance protein and the cystic fibrosis transmembrane conductance regulator. Int. Rev. Cytol. **137:**1–35.
2. **Baliarda, A., T. Robert, M. Jebbar, C. Blanco, A. Deschamps, and C. Le Marrec.** 2003. Potential osmoprotectans for the lactic acid bacteria *Pediococcus pentosaceus* and *Tetragenococcus halophila*. Int. J. Food Microbiol. **84:**13–20.
3. **Boch, J., B. Kempf, and E. Bremer.** 1994. Osmoregulation in *Bacillus subtilis*: synthesis of the osmoprotectant glycine betaine from exogenously provided choline. J. Bacteriol. **176:**5364–5371.
4. **Bremer, E.** 2002. Adaptation to changing osmolarity, p. 385–391. *In* A. L. Sonenshein, J. A. Hoch, and R. Losick (ed.), *Bacillus subtilis* and its closest relatives. ASM Press, Washington, DC.
5. **Bremer, E., and R. Krämer.** 2000. Coping with osmotic challenges: osmoregulation through accumulation and release of compatible solutes in bacteria, p. 79–97. *In* G. Storz and R. Hengge-Aronis (ed.), Bacterial stress responses. ASM Press, Washington, DC.
6. **Chambers, S. T., and C. M. Kunin.** 1987. Isolation of glycine betaine and proline betaine from human urine. J. Clin. Investig. **79:**731–737.
7. **Choquet, G., N. Jehan, C. Pissavin, C. Blanco, and M. Jebbar.** 2005. OusB, a broad-specificity ABC-type transporter from *Erwinia chrysanthemi*, mediates uptake of glycine betaine and choline with a high affinity. Appl. Environ. Microbiol. **71:**3389–3398.
8. **Collaborative Computational Project, Number 4.** 1994. The CCP4 suite: programs for protein crystallography. Acta Crystallogr. D **50:**760–763.
9. **Cosquer, A., V. Pichereau, J. A. Pocard, J. Minet, M. Cormier, and T. Bernard.** 1999. Nanomolar levels of dimethylsulfoniopropionate, dimethylsulfonioacetate, and glycine betaine are sufficient to confer osmoprotection to *Escherichia coli*. Appl. Environ. Microbiol. **65:**3304–3311.
10. **Diab, F., T. Bernard, A. Bazire, D. Haras, C. Blanco, and M. Jebbar.** 2006. Succinate-mediated catabolite repression control on the production of glycine betaine catabolic enzymes in *Pseudomonas aeruginos* PAO1 under low and elevated salinities. Microbiology **152:**1395–1406.
11. **Dougherty, D. A.** 1996. Cation-pi interactions in chemistry and biology: a new view of benzene, Phe, Tyr, and Trp. Science **271:**163–168.
12. **Emsley, P., and K. Cowtan.** 2004. Coot: model-building tools for molecular graphics. Acta Crystallogr. D **60:**2126–2132.
13. **Ferger, M. F., and V. Vigneaud.** 1950. Oxidation in vivo of the methyl groups of choline, betaine, dimethylthetin, and dimethyl-β-propiothetin. J. Biol. Chem. **185:**53–57.
14. **Hanekop, N., M. Hoing, L. Sohn-Bosser, M. Jebbar, L. Schmitt, and E. Bremer.** 2007. Crystal structure of the ligand-binding protein EhuB from *Sinorhizobium meliloti* reveals substrate recognition of the compatible solutes ectoine and hydroxyectoine. J. Mol. Biol. **374:**1237–1250.
15. **Harwood, C. R., and A. R. Archibald.** 1990. Growth, maintenance and general techniques, p. 1–26. *In* C. R. Harwood and S. M. Cutting (ed.), Molecular biological methods for *Bacillus*. John Wiley & Sons, Inc., Chichester, United Kingdom.
16. **Higgins, C. F.** 1992. ABC transporters: from microorganisms to man. Annu. Rev. Cell Biol. **8:**67–113.
17. **Horn, C., E. Bremer, and L. Schmitt.** 2005. Functional overexpression and in vitro assembly of OpuA, an osmotically regulated ABC-transporter from *Bacillus subtilis*. FEBS Lett. **579:**5765–5768.
18. **Horn, C., E. Bremer, and L. Schmitt.** 2003. Nucleotide dependent monomer/dimer equilibrium of OpuAA, the nucleotide-binding protein of the osmotically regulated ABC transporter OpuA from *Bacillus subtilis*. J. Mol. Biol. **334:**403–419.
19. **Horn, C., S. Jenewein, L. Sohn-Bosser, E. Bremer, and L. Schmitt.** 2005. Biochemical and structural analysis of the *Bacillus subtilis* ABC transporter OpuA and its isolated subunits. J. Mol. Microbiol. Biotechnol. **10:**76–91.
20. **Horn, C., L. Sohn-Bosser, J. Breed, W. Welte, L. Schmitt, and E. Bremer.** 2006. Molecular determinants for substrate specificity of the ligand-binding protein OpuAC from *Bacillus subtilis* for the compatible solutes glycine betaine and proline betaine. J. Mol. Biol. **357:**592–606.
21. **Jebbar, M., L. Sohn-Bosser, E. Bremer, T. Bernard, and C. Blanco.** 2005. Ectoine-induced proteins in *Sinorhizobium meliloti* include an ectoine ABC-type transporter involved in osmoprotection and ectoine catabolism. J. Bacteriol. **187:**1293–1304.
22. **Kappes, R. M., B. Kempf, and E. Bremer.** 1996. Three transport systems for the osmoprotectant glycine betaine operate in *Bacillus subtilis*: characterization of OpuD. J. Bacteriol. **178:**5071–5079.
23. **Kappes, R. M., B. Kempf, S. Kneip, J. Boch, J. Gade, J. Meier-Wagner, and E. Bremer.** 1999. Two evolutionarily closely related ABC transporters mediate the uptake of choline for synthesis of the osmoprotectant glycine betaine in *Bacillus subtilis*. Mol. Microbiol. **32:**203–216.
24. **Kempf, B., and E. Bremer.** 1995. OpuA, an osmotically regulated binding protein-dependent transport system for the osmoprotectant glycine betaine in *Bacillus subtilis*. J. Biol. Chem. **270:**16701–16713.
25. **Kempf, B., and E. Bremer.** 1998. Uptake and synthesis of compatible solutes as microbial stress responses to high-osmolality environments. Arch. Microbiol. **170:**319–330.
26. **Kempf, B., J. Gade, and E. Bremer.** 1997. Lipoprotein from the osmoregulated ABC transport system OpuA of *Bacillus subtilis*: purification of the glycine betaine binding protein and characterization of a functional lipidless mutant. J. Bacteriol. **179:**6213–6220.
27. **Kleywegt, G. J.** 1996. Use of non-crystallographic symmetry in protein structure refinement. Acta Crystallogr. D **52:**842–857.
28. **Kleywegt, G. J., and T. A. Jones.** 2002. Homo crystallographicus—quo vadis? Structure **10:**465–472.
29. **Ko, R., and L. T. Smith.** 1999. Identification of an ATP-driven, osmoregulated glycine betaine transport system in *Listeria monocytogenes*. Appl. Environ. Microbiol. **65:**4040–4048.
30. **Li, A. J., and R. Nussinov.** 1998. A set of van der Waals and coulombic radii of protein atoms for molecular and solvent-accessible surface calculation, packing evaluation, and docking. Proteins **32:**111–127.
31. **Ma, J. C., and D. A. Dougherty.** 1997. The cation-pi interaction. Chem. Rev. **97:**1303–1324.
32. **Mao, B., M. R. Pear, J. A. McCammon, and F. A. Quiocho.** 1982. Hinge-bending in L-arabinose-binding protein. The "Venus's-flytrap" model. J. Biol. Chem. **257:**1131–1133.
33. **Miller, J. H.** 1992. A short course in bacterial genetics: a laboratory manual and handbook for *Escherichia coli* and related bacteria. Cold Spring Harbor Laboratory Press, Cold Spring Harbor, NY.
34. **Murshudov, G., A. A. Vagin, and E. J. Dodson.** 1997. Refinement of macromolecular structures by the maximum-likelihood method. Acta Crystallogr. D **53:**240–255.
35. **Navaza, J.** 1994. AMoRe: an automated package for molecular replacement. Acta Crystallogr. D **50:**157–163.
36. **Obis, D., A. Guillot, J. C. Gripon, P. Renault, A. Bolotin, and M. Y. Mistou.** 1999. Genetic and biochemical characterization of a high-affinity betaine uptake system (BusA) in *Lactococcus lactis* reveals a new functional organization within bacterial ABC transporters. J. Bacteriol. **181:**6238–6246.
37. **Otwinowski, Z., and W. Minor.** 1997. Processing of X-ray diffraction data collected in oscillation mode. Methods Enzymol. **276:**307–326.
38. **Pichereau, V., J. A. Pocard, J. Hamelin, C. Blanco, and T. Bernard.** 1998. Differential effects of dimethylsulfoniopropionate, dimethylsulfonioacetate, and other S-methylated compounds on the growht of *Sinorhizobium meliloti* at low and high osmolarities. Appl. Environ. Microbiol. **64:**1420–1429.
39. **Quiocho, F. A., and P. S. Ledvina.** 1996. Atomic structure and specificity of bacterial periplasmic receptors for active transport and chemotaxis: variation of common themes. Mol. Microbiol. **20:**17–25.
40. **Schiefner, A., J. Breed, L. Bosser, S. Kneip, J. Gade, G. Holtmann, K. Diederichs, W. Welte, and E. Bremer.** 2004. Cation-pi interactions as determinants for binding of the compatible solutes glycine betaine and proline betaine by the periplasmic ligand-binding protein ProX from *Escherichia coli*. J. Biol. Chem. **279:**5588–5596.
41. **Schmidt, S., K. Pfluger, S. Kogl, R. Spanheimer, and V. Muller.** 2007. The salt-induced ABC transporter Ota of the methanogenic archaeon *Methanosarcina mazei* Go1 is a glycine betaine transporter. FEMS Microbiol. Lett. **277:**44–49.
42. **Schmitt, L., and R. Tampé.** 2002. Structure and mechanism of ABC-transporters. Curr. Opin. Struct. Biol. **12:**754–760.
43. **van der Heide, T., and B. Poolman.** 2002. ABC transporters: one, two or four extracytoplasmic substrate-binding sites? EMBO Rep. **3:**938–943.
44. **van der Heide, T., and B. Poolman.** 2000. Osmoregulated ABC-transport system of *Lactococcus lactis* senses water stress via changes in the physical state of the membrane. Proc. Natl. Acad. Sci. USA **97:**7102–7106.
45. **Wilkinson, A. J., and K. H. G. Verschueren.** 2003. Crystal structures of periplasmic solute binding proteins in ABC transport complexes illuminate their function. *In* I. B. Holland, S. P. Cole, and K. Kuchler (ed.), ABC proteins from bacteria to man. Academic Press, Amsterdam, The Netherlands.